ResearchGate

See discussions, stats, and author profiles for this publication at: https://www.researchgate.net/publication/51460000

Sulfur 1s near-edge x-ray absorption fine structure (NEXAFS) of thiol and thioether compounds

ARTICLE *in* THE JOURNAL OF CHEMICAL PHYSICS · JUNE 2011

Impact Factor: 2.95 · DOI: 10.1063/1.3602218 · Source: PubMed

CITATIONS
8

READS
35

3 AUTHORS, INCLUDING:

Shirin Behyan
University of British Columbia - Vancouver
8 PUBLICATIONS **42** CITATIONS
SEE PROFILE

Stephen G Urquhart
University of Saskatchewan
84 PUBLICATIONS **1,737** CITATIONS
SEE PROFILE

Available from: Shirin Behyan
Retrieved on: 26 January 2016

Sulfur 1s near-edge x-ray absorption fine structure (NEXAFS) of thiol and thioether compounds

Shirin Behyan, Yongfeng Hu, and Stephen G. Urquhart

Citation: J. Chem. Phys. **134**, 244304 (2011); doi: 10.1063/1.3602218
View online: http://dx.doi.org/10.1063/1.3602218
View Table of Contents: http://jcp.aip.org/resource/1/JCPSA6/v134/i24
Published by the American Institute of Physics.

Additional information on J. Chem. Phys.

Journal Homepage: http://jcp.aip.org/
Journal Information: http://jcp.aip.org/about/about_the_journal
Top downloads: http://jcp.aip.org/features/most_downloaded
Information for Authors: http://jcp.aip.org/authors

ADVERTISEMENT

Downloaded 21 Feb 2012 to 128.233.108.204. Redistribution subject to AIP license or copyright; see http://jcp.aip.org/about/rights_and_permissions

Sulfur 1*s* near-edge x-ray absorption fine structure (NEXAFS) of thiol and thioether compounds

Shirin Behyan,[1] Yongfeng Hu,[2] and Stephen G. Urquhart[1,a)]
[1]*Department of Chemistry, University of Saskatchewan, Saskatoon, Saskatchewan S7N 5C9, Canada*
[2]*Canadian Light Source, University of Saskatchewan, Saskatoon, Saskatchewan S7N 5C6, Canada*

(Received 14 February 2011; accepted 2 June 2011; published online 27 June 2011; corrected 16 November 2011)

The speciation and quantification of sulfur species based on sulfur K-edge x-ray absorption spectroscopy is of wide interest, particularly for biological and petroleum science. These tasks require a firm understanding of the sulfur 1*s* near-edge x-ray absorption fine structure (NEXAFS) spectra of relevant species. To this end, we have examined the gas phase sulfur 1*s* NEXAFS spectra of a group of simple thiol and thioether compounds. These high-resolution gas phase spectra are free of solid-state broadening, charging, and saturation effects common in the NEXAFS spectra of solids. These experimental data have been further analyzed with the aid of improved virtual orbital Hartree–Fock *ab initio* calculations. The experimental sulfur 1*s* NEXAFS spectra show fine features predicted by calculation, and the combination of experiment and calculation has been used to improve assignment of spectroscopic features relevant for the speciation and quantification of the sulfur compounds.
© *2011 American Institute of Physics*. [doi:10.1063/1.3602218]

INTRODUCTION

The refinement of analytical methods for sulfur speciation, particularly microanalytical methods, is of great interest for the study of energy and fuels, industrial processes and products, biological systems, and other complex materials. Near-edge x-ray absorption fine structure (NEXAFS) spectroscopy is ideal for studying the form and quantity of sulfur species. In contrast, nuclear magnetic resonance (NMR) spectroscopy is relatively inefficient, as the NMR active isotope, ^{33}S, has a low natural abundance (0.76%) and its quadruple spin ($I = 3/2$) leads to weak and broad signals.[1] NEXAFS spectroscopy, at the sulfur 2*p* (162 eV) and the sulfur 1*s* (2472 eV) core edges, is frequently used for speciation and quantification of sulfur. For example, sulfur 1*s* NEXAFS has been used to determine the ratio of thiols to disulfides in biological systems; this difference affects the functionality of many proteins.[2] Deconvolution of complex sulfur 1*s* spectra has also been used for speciation in biological systems.[3,4] Sulfur speciation is also important in solid oxide fuel cells, where deactivation occurs as trace sulfur in fuels reacts with the nickel catalyst in the anodes.[5] One of the factors determining the fossil fuel quality is the quantity and form of the sulfur compounds. As the combustion of these compounds produces sulfur dioxide and decreases the performance of catalytic converters, low sulfur fuel standards have been mandated. Sulfur 1*s* NEXAFS has been used for speciation and quantification of sulfur compounds in fossil fuel,[6] studies of the surface adsorption of thiols and thiolates,[7,8] and the sulfur chemistry of polymers[9] and photographic materials.[10]

Developments in x-ray microprobe and zone plate microscopies allow for sulfur 1*s* NEXAFS spectra to be acquired from yet smaller sample volumes,[11] extending this spectroscopy as a microanalytical method. In sequence with the development of sulfur 1*s* NEXAFS spectroscopy capabilities at the scanning transmission x-ray microscopy at the Canadian Light Source (CLS)[12] and the potential for studies of sulfur in asphaltene species from the Canadian oil sands and lignite coal deposits in south-eastern Saskatchewan, we are exploring the basic interpretation of the sulfur 1*s* NEXAFS spectra.

In this paper, we focus on the simplest organosulfur species, thiols and thioethers, to provide a baseline for studies of complex sulfur species expected in asphaltenes. The sulfur 1*s* NEXAFS spectra of simple thiols and thioether compounds have been previously assigned by empirical comparisons[3,7,13,14] and some recent calculations.[15–18]

There have been relatively few theoretical studies of sulfur 1*s* NEXAFS spectra of organosulfur compounds until relatively recently.[15–21] Nakamatsu *et al*. examined the sulfur 1*s* and sulfur 2*p* NEXAFS spectra of SF_6 and H_2S (relevant for considering S–H/thiol bonding) by discrete variational (DV)-Xα calculations and assigned spectroscopic features in terms of transitions to specific unoccupied molecular orbitals.[19] Sarangi *et al*. examined density functional theory (DFT) simulations of the sulfur 1*s* NEXAFS spectra of species that represent S–CH_3 and S–S bonding as well as the sulfite group and observed chemical bonding effects in addition to anticipated oxidation state effects.[16] Mijovilovich *et al*. simulated the sulfur 1*s* NEXAFS spectra for sulfides and disulfides by DFT calculations and showed that significant spectroscopic differences arise from sulfur-sulfur bonding and the nature of ligand groups attached to a sulfur atom (phenyl versus benzyl, etc.).[15] Mijovilovich *et al*. have compared the experimental sulfur 1*s* NEXAFS spectra of dibenzothiophene, dibenzothiophene sulfone, and DL-methionine to calculations at several different levels of

a)Author to whom correspondence should be addressed. Electronic mail: stephen.urquhart@usask.ca.

 © 2011 American Institute of Physics

Downloaded 21 Feb 2012 to 128.233.108.204. Redistribution subject to AIP license or copyright; see http://jcp.aip.org/about/rights_and_permissions

DFT theory.[17] From the similar "white line" energy in the spectra of different molecules, the authors suggest that the "fingerprint" resolution of compounds will be difficult.[17]

Recently, the effect of solvation and coordination on sulfur 1*s* spectra have also been considered.[22] Risberg *et al*. studied the role of external interactions, such as hydrogen bonding, deprotonation, and complexation, on sulfur-containing amino acids and oxidation products by the transition potential DFT method.[18] This work demonstrates that spectroscopic models must reflect the chemical surroundings of the materials they seek to model. Damian *et al*. simulated the NEXAFS spectra of dimethyl sulfoxide (DMSO) in the solvated Thallium(III), Indium(III), Gallium (III), and Aluminum(III) solutions and concluded that increased splitting of the sulfur 1*s* spectra is due to metal/oxygen orbital interactions between the coordinated DMSO ligand and the metal ion.[21] Other theoretical studies have addressed mineral, oxyanion, and oxide forms of sulfur[22–24] and halogenated sulfur species.[20,25]

A common theme of this recent work is the great sensitivity of sulfur 1*s* spectroscopy to fine differences in structure, bonding, and intermolecular interactions. This spectroscopic sensitivity variation is not only useful for analytical studies but also creates a substantial risk for chemical misassignment when poorly understood spectra are used, particularly when features from different chemical moieties appear in the same energy range.

This work examines simple compounds in the gas phase and compares these to a wider range of *ab initio* calculations, from simple to complex species. Gas phase spectra are free of solid-state broadening, charging in the total electron yield (TEY) detection of solids, and self-absorption present in fluorescent yield detection. We have examined the calculated sulfur 1*s* NEXAFS spectra from *ab initio* improved virtual orbital (IVO) calculations of thiols and thioethers of different complexities, such as simple thiols (hydrogen sulfide, methanethiol, and ethanethiol), a simple aromatic thiol (benzenethiol), simple aliphatic thioethers (dimethyl sulfide and methionine), and the aliphatic cyclo-thioether tetrahydrothiophene (see Scheme 1).

Molecular structure	Name
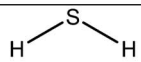	Hydrogen sulfide
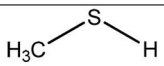	Methanethiol
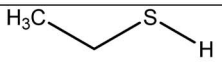	Ethanethiol
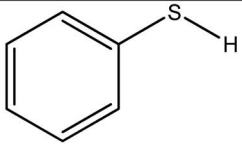	Benzenethiol
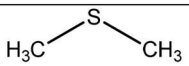	Dimethyl sulfide
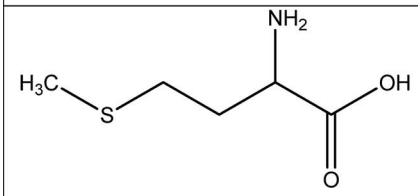	Methionine
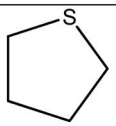	Tetrahydrothiophene

SCHEME 1. Molecular drawings of thiols and thioethers.

COMPUTATIONAL METHODS

Ab initio calculations were carried out by Kosugi's GSCF3 package.[26] This approach is based on the *ab initio* improved virtual orbital (IVO) approximation, which explicitly includes the core hole in the Hartree–Fock Hamiltonian. The IVO approximation is effective at the simulation of core excitation spectra of organic and organometallic compounds.[27–31] The IVO approximation has been widely employed to calculate the NEXAFS spectra of organic compounds at the carbon, nitrogen, oxygen, and silicon 1*s* edges.[26,27,29,32,33] On this basis, it is natural to expect a similar success for organosulfur compounds. IVO calculations are particularly effective for transitions below and near the ionization potential (IP), where the sulfur 1*s* NEXAFS spectra show the strongest and most distinctive transitions.

The geometries used for these calculations (see Scheme 1) were provided by *ab initio* geometry optimization at the HF/6-31G* level, by the SPARTAN 06 program.[34] Frequency calculations were performed to ensure that the geometries were minimum structures (no imaginary frequencies). For the IVO calculations with GSCF3, we used similar basis sets to that used for organosilicon compounds:[30] Hydrogen (41); second row atoms (carbon, nitrogen, and oxygen) (621 41); sulfur (with the core hole) (311111111 311111), with an additional *d* polarization function on the sulfur atom ($\zeta_d = 0.421$).

Simulated spectra were obtained from the IVO calculations by broadening each transition as a Gaussian line with the SIMILE2 package,[35] with the following energy dependent widths: 0.6 eV FWHM for bound states, 1.2 eV FWHM for states from the ionization potential to 4 eV above the IP, and 4.0 eV FWHM for states more than 4.0 eV above the IP. These widths are chosen to approximately track the experimental line width observed in the sulfur 1*s* NEXAFS spectra, but where the bound states are somewhat narrower than experiment so that fine spectroscopic differences can be more readily observed.[29,30,33] MO plots are provided for selected unoccupied orbitals.

EXPERIMENTAL

All compounds (ethanethiol 97%, tetrahydrothiophene 99%, DL-methionine ≥ 99%, and benzenethiol ≥ 99%) were

Downloaded 21 Feb 2012 to 128.233.108.204. Redistribution subject to AIP license or copyright; see http://jcp.aip.org/about/rights_and_permissions

of reagent grade and purchased from Sigma Aldrich with the exception of dimethyl sulfide (98%), which was purchased from Alfa Aesar.

Experimental spectra of the gas phase molecules as well as the solid phase DL-methionine were obtained at the Canadian Light Source on soft x-ray microcharacterization beamline (SXRMB), using a Si (1 1 1) crystal monochromator which provides an energy resolution of 0.24 eV. The gas samples were introduced into a double gas cell (two gas cells in sequence) from the vapour pressure of the pure samples. The pressure inside the gas cell was in the range of 9.9–13.9 mTorr, below the pressure onset of saturation effects. The absence of saturation was also verified by comparing the spectra from the first and second gas cells.

The experimental spectra of the gas phase molecules were recorded with total ion yield (TIY) detection mode.[36] For DL-methionine, the fine powder was spread homogeneously on the sulfur free carbon tape and its NEXAFS spectrum was measured with total electron yield and fluorescence detection. The TIY and TEY NEXAFS spectra were normalized by dividing each spectrum by a simultaneously recorded Io spectrum from an ion chamber upstream from the sample gas cell.

The energy scale was calibrated to an absolute energy scale instead of an agreed energy of a standard. This was done by setting the energy of the Ar $1s \rightarrow 4p$ transition to the value of 3203.54 (10) eV, based on the absolute energy calibration of Breinig *et al*.[37] In our experiments, the Ar $1s \rightarrow 4p$ transition energy was used to calibrate a weak contaminant signal (presumably from $FeSO_4$ contamination) found on the Be windows of the ion chamber (calibrated value, 2481.62 eV). This signal, recorded at the same time as all other spectra, was used as an internal calibration for our experiments. On this scale, the white line of the $ZnSO_4$ appears at 2481.47 eV, which is well within experimental error of the 2481.44 eV value reported in the literature.[17] The accuracy of this calibration is estimated to be ±0.3 eV, based on the ~0.7 eV life-time broadening of the Ar $1s \rightarrow 4p$ transition. (See supplementary material for a summary of literature calibrations at the sulfur 1*s* energy.)[38]

In comparing the experimental spectra to the calculated (IVO) spectra, the calculated spectra always appear at lower energy than the experimental spectra (4.62 eV lower energy for thiols and 4.47 eV in aliphatic thioethers). IVO spectra for second row species usually appear at higher energy than the corresponding experimental spectra,[27,28,30] but strong relativistic effects for higher Z (third row) species, lead to a shift in the opposite direction.[21–23] For example, in DFT calculations by Risberg *et al*., the S 1*s* ionization potential increased by 7.4 eV when relativistic terms are included.[22] In this paper, we present experimental data on the calibrated energy scale, and the theoretical data on their calculated energy scales.

RESULTS AND DISCUSSION

In this section, experimental sulfur 1*s* NEXAFS spectra are compared to the simulated sulfur 1*s* NEXAFS spectra of a series of thiols and thioethers. The sensitivity of the NEXAFS spectra is explored in more detail below.

Thiols

Figure 1(a) examines the simulated sulfur 1*s* NEXAFS spectra of hydrogen sulfide (H_2S), methanethiol (CH_3SH), ethanethiol (C_2H_5SH), and benzenethiol (C_6H_5SH) and compares these spectra with the experimental sulfur 1*s* spectra of ethanethiol and benzenethiol. Figure 1(b) presents MO plots of the unoccupied orbitals of the most intense pre-edge features in these spectra. Table I presents the calculated energies, term values (term value = ionization potential − transition energy), ionization potentials, and transition character for the features appearing below the ionization potential. Table II presents the experimental energies and assignments for these transitions.

The experimental sulfur 1*s* NEXAFS spectra of ethanethiol and benzenethiol show higher resolution than the previous results, now clearly showing the splitting in the white line.[13] We observe that the white line and the higher energy shoulder (peaks 1 and 2) in benzenethiol move to higher energy than in ethanethiol. This can be ascribed to the inductive effect of the phenyl ring, which depletes the electron density on the sulfur atom and increases the sulfur 1*s* binding energy.

The simulated spectra and molecular orbitals show that the most intense feature in the sulfur 1*s* NEXAFS spectrum of hydrogen sulfide is formed from two nearly degenerate transitions. MO diagrams show that these transitions are to σ^*(S–H) unoccupied orbitals corresponding to the b_1 (LUMO) and a_1 (LUMO + 1) symmetry representations within the C_{2v} point group for H_2S.

Relative to hydrogen sulfide, we expect additional σ^*(S–C) unoccupied orbital character in the sulfur 1*s* spectrum of

TABLE I. Calculated energies, term values, ionization potentials, and assignments for sulfur 1*s* transitions appearing below the ionization potential for hydrogen sulfide, methanethiol, and benzenethiol from *ab initio* IVO calculations.

#	Energy (eV)	Term value (eV)	Oscillator strength	Assignment
Hydrogen sulfide ionization potential: 2471.37 eV				
LUMO	2467.47	3.898	0. 003524	S $1s \rightarrow \sigma^*$(S–H)
LUMO + 1	2467.51	3.860	0.001473	S $1s \rightarrow \sigma^*$(S–H)
Methanethiol ionization potential: 2470.54 eV				
LUMO	2467.32	3.221	0.002621	S $1s \rightarrow \sigma^*$(S–H)
				Weak S $1s \rightarrow \sigma$(S–C)
LUMO + 1	2468.29	2.250	0.001510	S $1s \rightarrow \sigma^*$(S–C)
LUMO + 2	2470.29	0.252	0.0006318	Poorly defined
Ethanethiol ionization potential: 2470.28 eV				
LUMO	2467.30	2.987	0.002665	S $1s \rightarrow \sigma^*$(S–H)
				Weak S $1s \rightarrow \sigma$ (S–C)
LUMO + 1	2468.52	1.766	0.001267	S $1s \rightarrow \sigma^*$(S–C)
LUMO + 2	2470.09	0.193	0.0004423	Poorly defined
Benzenethiol ionization potential: 2470.42 eV				
LUMO	2467.57	2.842	0.002008	S $1s \rightarrow \sigma^*$(S–H)
				Weak S $1s \rightarrow \sigma$ (S–C)
LUMO + 1	2468.83	1.583	0.0006201	S $1s \rightarrow \pi^*$(C=C) weak
LUMO + 2	2469.13	1.289	0.001485	S $1s \rightarrow \sigma^*$(S–C)

Downloaded 21 Feb 2012 to 128.233.108.204. Redistribution subject to AIP license or copyright; see http://jcp.aip.org/about/rights_and_permissions

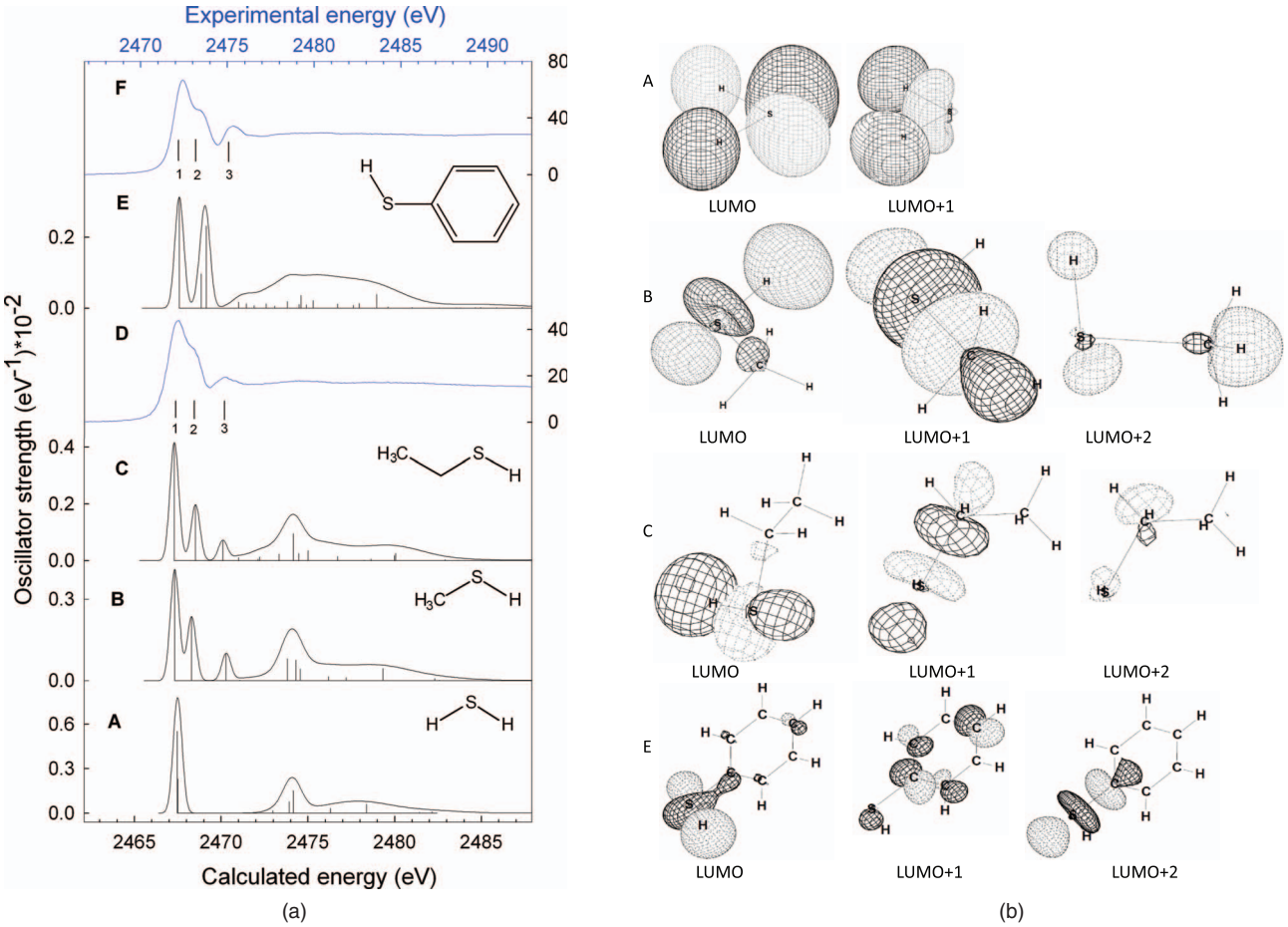

FIG. 1. (a) Comparison of experimental gas phase sulfur 1*s* NEXAFS spectra, recorded by total ion yield, to the predicted sulfur 1*s* spectra from *ab initio* IVO calculations. A: calculated spectra of hydrogen sulfide; B: calculated spectrum of methanethiol; C: calculated spectrum of ethanethiol; D: experimental spectrum of ethanethiol; E: calculated spectrum of benzenethiol; F: experimental spectrum of benzenethiol. The experimental energy scale (shown on the top of graph) is shifted relative to the calculated energy scale (shown at the bottom). (b) Unoccupied molecular orbital diagrams for the strong features contributing to the simulated spectra. A: Hydrogen sulfide; B: methanethiol; C: ethanethiol; and E: benzenethiol.

TABLE II. Transition energies for the experimental sulfur 1*s* NEXAFS spectra of ethanethiol, benzenethiol, dimethyl sulfide, DL-methionine, and tetrahydrofuran, recorded using total ion yield detection.[a]

Compound name	Feature #	Energy (eV)
Ethanethiol	1	2472.17
	2	2473.11
	3	2474.87
Benzenethiol	1	2472.42
	2	2473.47
	3	2475.33
Dimethyl sulfide	1	2472.60
	2	2473.23
	3	2474.70
DL-methionine	1	2472.62
	2	2473.41
	3	2475.14
Tetrahydrothiophene	1	2472.23
	2	2473.31
	3	2474.24

[a]Spectra calibrated by setting the white line of the sulfate contamination in the Io signal to 2481.62 eV. See text for a discussion of the calibration procedure.

methanethiol. The simulations predict that the LUMO is predominantly a sulfur $1s \rightarrow \sigma^*$(S–H) character, with a small, poorly defined sulfur $1s \rightarrow \sigma^*$(S–C) contribution. In contrast, the LUMO + 1 is entirely a sulfur $1s \rightarrow \sigma^*$(S–C) character. Surprisingly, the two transitions have almost completely separated sulfur $1s \rightarrow \sigma^*$(S–H) and sulfur $1s \rightarrow \sigma^*$(S–C) characters. A similar observation is made for ethanethiol. However, the second transition is not fully resolved in the experimental sulfur 1*s* spectrum of ethanethiol and appears as a higher energy shoulder on the main peak at 2473.11 eV (peak 2).

A third peak (LUMO + 2) in methanethiol and ethanethiol appears at slightly higher energy in the calculated spectra; this is associated with the feature (peak 3) at a similar position in the experimental sulfur 1*s* NEXAFS spectrum of ethanethiol at 2474.87 eV. This feature cannot be easily assigned to a specific antibonding orbital, and the LUMO has σ^*(S–H) and σ (S–C) characters.

These assignments differ somewhat from those in the literature, where the first peak (1) in the experimental ethanethiol was assigned as a sulfur $1s \rightarrow \sigma^*$(S–C) transition, the higher energy shoulder (2) was not resolved, and the third energy peak (3) was assigned as a sulfur 1*s*

Downloaded 21 Feb 2012 to 128.233.108.204. Redistribution subject to AIP license or copyright; see http://jcp.aip.org/about/rights_and_permissions

$\rightarrow \sigma^*$(S–H)/4*p* transition.[13] Our new calculations clearly show that separate and resolvable sulfur $1s \rightarrow \sigma^*$(S–C) and the sulfur $1s \rightarrow \sigma^*$(S–H) transitions contribute to the main peak.

In benzenethiol, the first transition is predominantly a sulfur $1s \rightarrow \sigma^*$(S–H) character with some small but poorly defined sulfur $1s \rightarrow \sigma$(S–C) character, similar to the other thiols. The second transition (corresponding to the LUMO + 1) is relatively weak, and this transition samples the π^* density in the phenyl ring. Similar π^* interactions were observed by Mijovilovich *et al*. in the sulfur 1*s* spectra of phenyl benzyl sulfide.[15] The transition to the LUMO + 2 is stronger with sulfur $1s \rightarrow \sigma^*$(S–C) character, similar to the LUMO + 1 in methanethiol and ethanethiol. In the previous assignments for the sulfur 1*s* spectrum of benzenethiol, the main peak (1) and its high energy shoulder (2) were assigned as sulfur $1s \rightarrow \sigma^*$(S–C) and sulfur $1s \rightarrow 4s$, respectively.[13] Our results show that the main peak has sulfur $1s \rightarrow \sigma^*$(S–H) and σ(S–C) characters. The sulfur $1s \rightarrow \sigma^*$(S–H) contribution occurs in the first strong peak and not at higher energy as previously assigned.[13] The higher energy shoulders in benzenethiol contains a transition with clear sulfur $1s \rightarrow \sigma^*$(S–C) character (LUMO + 2), while the LUMO + 1 transition cannot be assigned to a simple orbital symmetry

Overall, these results show differentiated sulfur $1s \rightarrow \sigma^*$(S–H) and sulfur $1s \rightarrow \sigma^*$(S–C) transitions, closely spaced in energy and resolvable. The first transition in the aliphatic thiols is not a pure σ^*(S–H), but includes some σ(S–C) characters.

In the calculated NEXAFS spectra, the first transition energies of the aliphatic thiols behave as follows: benzenethiol > hydrogen sulfide > methanethiol ≈ ethanethiol. The difference in the first transition energy from methanethiol to ethanethiol is only 0.02 eV but the difference is 0.26 eV between benzenethiol to methanethiol. The same trend is observed in the experimental sulfur 1*s* spectra of benzenethiol and ethanethiol. This result shows that the benzene group has a larger effect than the aliphatic groups in the first energy transition.

Thioethers

Figure 2(a) presents the simulated sulfur 1*s* NEXAFS spectra of three aliphatic thioethers, dimethyl sulfide, methionine, and tetrahydrothiophene and compares these spectra with their experimental sulfur 1*s* spectra. Figure 2(b) presents MO plots of the unoccupied orbitals corresponding to the most intense pre-edge features in these spectra. Table II presents the energies and assignments from the experimental sulfur 1*s* spectra. Table III presents the calculated energies, term values, ionization potentials, and transition character for the features that appear below the ionization potential.

The sulfur 1*s* NEXAFS spectrum of methionine is similar to that previously published,[17] while the new gas phase spectrum of dimethyl sulfide is improved relative to the literature,[13] showing a clearer definition of the higher energy shoulder in the main peak. The experimental sulfur 1*s* spectra of dimethyl sulfide and DL-methionine have an intense transition with a higher energy shoulder and weak features at higher energy. Two slightly separated sulfur $1s \rightarrow \sigma^*$(S–C) transitions (see discussion of assignments, below) contribute to the intense feature. However, a greater splitting is observed in the DL-methionine for the sulfur $1s \rightarrow \sigma^*$(S–C) transitions, perhaps due to the inductive effect of amino acid group on the molecular orbital with strong σ^*(S–C) character, relative to the two other thioethers. In tetrahydrothiophene, the single intense feature makes the experimental white line appear narrower, with a weaker higher energy shoulder at 2473.31 eV (peak 2).

TABLE III. Calculated energies, term values, ionization potentials, and assignments for sulfur 1*s* transitions. Appearing below are the ionization potentials for tetrahydrothiophene, dimethyl sulfide, methionine, and tetrahydrothiophene from *ab initio* calculations.

#	Energy (eV)	Term value (eV)	Oscillator strength	Assignment
Dimethyl sulfide ionization potential: 2469.94 eV				
LUMO	2468.07	1.876	0.002644	S $1s \rightarrow \sigma^*$(S–C)
LUMO + 1	2468.91	1.039	0.001285	S $1s \rightarrow \sigma^*$(S–C)
LUMO + 2	2469.01	0.937	0.0000945	S $1s \rightarrow \sigma^*$(S–C)
Methionine ionization potential: 2470.01 eV				
LUMO	2468.24	1.769	0.002514	S $1s \rightarrow \sigma^*$(S–C)
LUMO + 1	2468.99	1.025	0.001279	S $1s \rightarrow \sigma^*$(S–C)
LUMO + 2	2469.25	0.765	0.0000078	S $1s \rightarrow \sigma^*$(S–C)
Tetrahydrothiophene ionization potential: 2469.47 eV				
LUMO	2467.82	1.659	0.002791	S $1s \rightarrow \sigma^*$(S–C)
LUMO + 1	2468.67	0.806	0.0004623	S $1s \rightarrow \sigma^*$(S–C)
LUMO + 2	2469.15	0.323	0.0004886	S $1s \rightarrow \sigma^*$(S–C)

In the simulated NEXAFS spectrum of dimethyl sulfide, the main transition is formed from two adjacent transitions, each with a sulfur $1s \rightarrow \sigma^*$(S–C) character. These features correspond to the b_1 (LUMO) and a_1 (LUMO + 1) features observed in H_2S, consistent with the C_{2v} symmetry in these species. A comparison to Figure 1(a) illustrates a clear trend from hydrogen sulfide (H_2S), methanethiol (CH_3SH) to dimethyl sulfide, $(CH_3)_2S$, as the orbital character changes from nearly degenerate σ^*(S–H), mixed σ^*(S–C) and σ^*(S–H), to adjacent transitions of σ^*(S–C) character.

Methionine is very similar to dimethyl sulfide, which is not surprising as the sulfur has a similar thioether environment in both cases. The MO plots are similar, with a decrease in symmetry relative to dimethyl sulfide. On this basis, one expects the sulfur 1*s* spectrum of methionine to be similar to $CH_3SCH_2CH_3$ or $CH_3SCH_2CH_2CH_3$, e.g., as an asymmetric dialkyl thioether. Tetrahydrothiophene has a cyclic thioether environment, and a different pattern of sulfur $1s \rightarrow \sigma^*$(S–C) transitions; one intense transition and two weaker transitions at slightly higher energy.

The energy order of the first transition in the simulated spectra is as follows: tetrahydrothiophene < dimethylsulfide < methionine. As seen in Table III, the position of these features correlate with the sulfur 1*s* ionization potential, reflecting slight differences in the inductive

Downloaded 21 Feb 2012 to 128.233.108.204. Redistribution subject to AIP license or copyright; see http://jcp.aip.org/about/rights_and_permissions

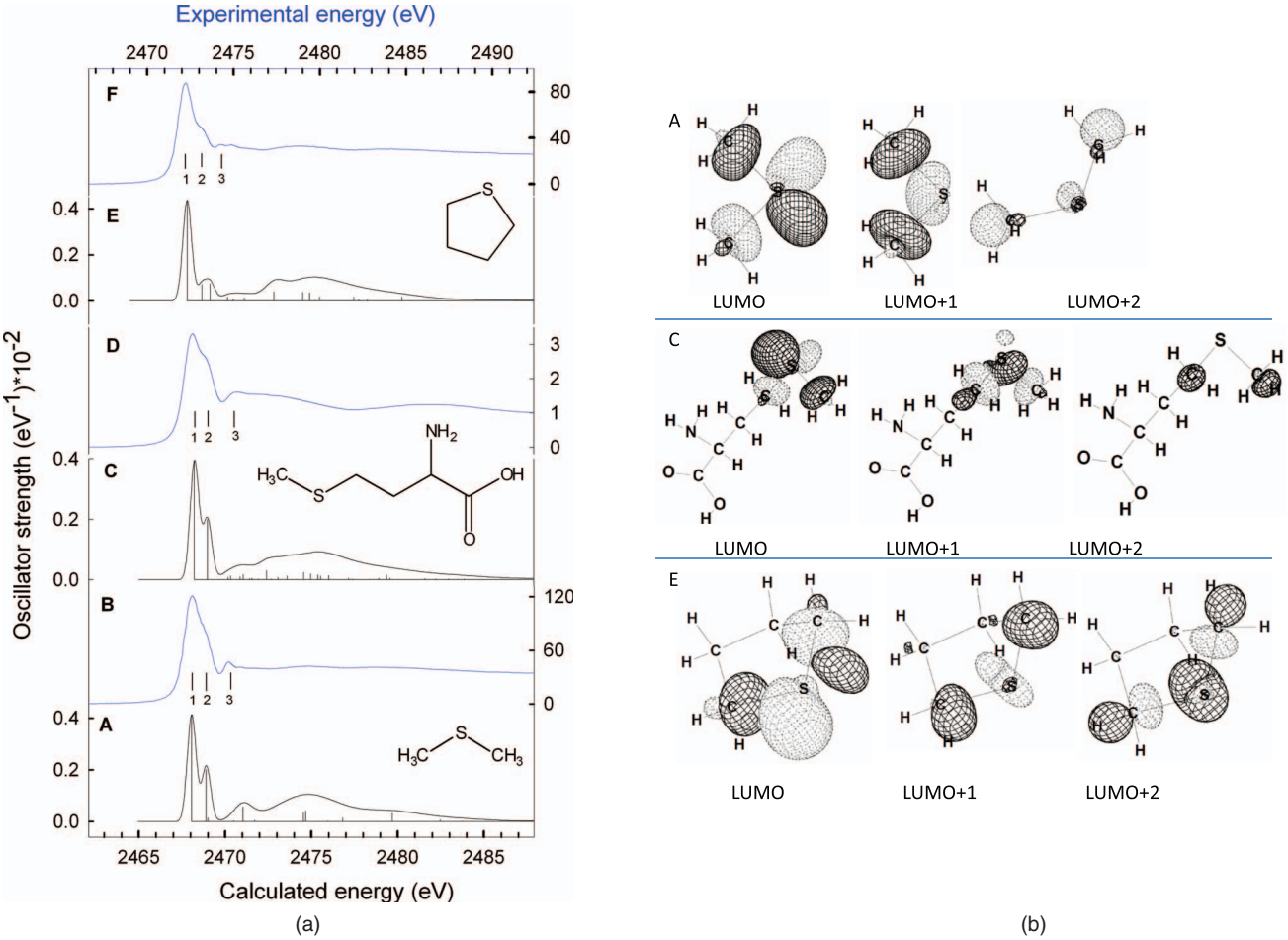

FIG. 2. (a) Comparison of experimental gas phase sulfur 1*s* NEXAFS spectra, recorded by total ion yield, to the predicted sulfur 1*s* spectra from *ab initio* IVO calculations. A: calculated spectrum of dimethyl sulfide; B: experimental spectrum of dimethyl sulfide; C: calculated spectrum of methionine; D: experimental spectrum of DL-methionine in solid phase; E: calculated spectrum of tetrahydrothiophene; F: experimental spectrum of tetrahydrothiophene. The experimental energy scale (shown on the top of graph) is shifted relative to the calculated energy scale (shown at the bottom). (b) Unoccupied molecular orbital diagrams for the strong features contributing to the simulated spectra. A: dimethyl sulfide; C: methionine; E: tetrahydrothiophene.

environment of the thioether substituent. The lower energy transition of the white line in tetrahydrothiophene can be ascribed to the heterocyclic ring tension. The experimental spectra are well reproduced by the calculations, and the order of the white line energies are also in agreement with the calculations.

CONCLUSION

In this study, the sulfur 1*s* NEXAFS spectra of a group of simple thiol and thioether molecules were studied by experiment and computational methods. The spectra of thiols are dominated by sulfur $1s \rightarrow \sigma^*$(S–H) and sulfur $1s \rightarrow \sigma^*$(S–C) transitions. These features are closely spaced in energy, and the higher energy sulfur $1s \rightarrow \sigma^*$(S–H) transition can be resolved as a shoulder in our high energy resolution gas phase spectra of the thiols. In benzenethiol, a π^*(C=C) transition also contributes to the higher energy shoulder. The white line energy in the thiol spectra is partly determined by the ligand groups attached to the sulfur atom, with a stronger effect from the phenyl group than from the aliphatic groups. Therefore, the speciation of the aliphatic thiols can be problematic due to feature overlap.

In aliphatic thioethers, the main peak in experimental spectra is composed of several closely spaced σ^*(S–C) character transitions, and the white line transition energy is affected by the ligand groups attached to the sulfur atom. The shapes of the spectra of the non-cyclic thioethers are similar, while that of the cyclic thioether (tetrahydrothiophene) differ. The inductive effect of the amino acid group may be responsible for the small differences in the non-cyclic thioether compounds, and the cyclic strain in tetrahydrothiophene determines the relative intensity of the σ^*(S–C) transitions.

The comparison between theory and experiment is excellent. The best selected DFT methods, such as the half-core hole approximation calculations,[17] are comparable to our standard *ab initio* IVO calculation results. Our high resolution gas phase data shows improved energy resolution relative to that previously published. These data are also free from solid-state broadening and common detection artefacts, providing an excellent comparison to theory. This allows us to identify the character of analytically useful transitions in the NEXAFS spectra of organosulfur molecules.

Downloaded 21 Feb 2012 to 128.233.108.204. Redistribution subject to AIP license or copyright; see http://jcp.aip.org/about/rights_and_permissions

For speciation, care must be taken to avoid simplistic σ^*(S–H) and σ^*(S–C) assignments and spectroscopic interpretation as both σ^*(S–H) and σ^*(S–C) orbital characters contribute to the white line in thiol and thioether molecules. Shifts in the energy of these features are apparent: thioethers appear at slightly higher energy than thiols; however, strained systems, such as tetrahydrothiophene, show the white line closer to thiol energies. As in all analytical studies, evidence from NEXAFS spectroscopy must be weighed together with other information about a complex sample to either narrow the range of possible chemical composition or to make specific composition assignments where warranted.

ACKNOWLEDGMENTS

S.G.U. is funded by NSERC (Canada). Research described in this paper was performed at the Canadian Light Source, which is supported by the Natural Sciences and Engineering Research Council of Canada, the National Research Council Canada, the Canadian Institutes of Health Research, Saskatchewan, Western Economic Diversification Canada, and the University of Saskatchewan.

[1]F. Jalilehvand, Chem. Soc. Rev. **35**(12), 1256 (2006).
[2]A. Rompel, R. M. Cinco, M. J. Latimer, A. E. McDermott, R. D. Guiles, A. Quintanilha, R. M. Krauss, K. Sauer, V. K. Yachandra, and M. P. Klein, Proc. Natl. Acad. Sci. U.S.A. **95**(11), 6122 (1998).
[3]A. Prange, C. Dahl, H. G. Truper, M. Behnke, J. Hahn, H. Modrow, and J. Hormes, Eur. Phys. J. D **20**, 589 (2002); I. J. Pickering, R. C. Prince, T. Divers, and G. N. George, FEBS Lett. **441**(1), 11 (1998).
[4]I. J. Pickering, G. N. George, E. Y. Yu, D. C. Brune, C. Tuschak, J. Overmann, J. T. Beatty, and R. C. Prince, Biochemistry **40**(27), 8138 (2001); P. Frank, B. Hedman, and K. O. Hodgson, Inorg. Chem. **38**(2), 260 (1999).
[5]A. Braun, M. Janousch, J. Sfeir, J. Kiviaho, M. Noponen, F. E. Huggins, M. J. Smith, R. Steinberger-Wilckens, P. Holtappels, and T. Graule, J. Power Sources **183**(2), 564 (2008).
[6]S. Matsumoto, Y. Tanaka, H. Ishii, T. Tanabe, Y. Kitajima, and J. Kawai, Spectrochim. Acta, Part B **61**(8), 991 (2006); R. Wiltfong, S. Mitra-Kirtley, O. C. Mullins, B. Andrews, G. Fujisawa, and J. W. Larsen, Energy Fuels **19**(5), 1971 (2005); G. Sarret, J. Connan, M. Kasrai, G. M. Bancroft, A. Charrié-Duhaut, S. Lemoine, P. Adam, P. Albrecht, and L. Eybert-Bérard, Geochim. Cosmochim. Acta **63**(22), 3767 (1999); G. N. George, M. L. Gorbaty, S. R. Kelemen, and M. Sansone, Energy Fuels **5**(1), 93 (1991); G. N. George and M. L. Gorbaty, J. Am. Chem. Soc. **111**(9), 3182 (1989); G. Almkvist, K. Boye, and I. Persson, J. Synchrotron Radiat. **17**, 683 (2010).
[7]F. Allegretti, F. Bussolotti, D. P. Woodruff, V. R. Dhanak, M. Beccari, V. Di Castro, M. G. Betti, and C. Mariani, Surf. Sci. **602**(14), 2453 (2008).
[8]S. A. Sardar, J. A. Syed, S. Yagi, and K. Tanaka, Thin Solid Films **450**(2), 265 (2004); J. A. Syed, S. A. Sardar, S. Yagi, and K. Tanaka, Surf. Sci. **566**, 597 (2004); J. A. Syed, S. A. Sardar, S. Yagi, and K. Tanaka, J. Vac. Sci. Technol. A **22**(3), 683 (2004); J. A. Syed, S. A. Sardar, S. Yagi, and K. Tanaka, Thin Solid Films **515**(4), 2130 (2006).
[9]H. Modrow, G. Calderon, W. H. Daly, G. G. B. de Souza, R. C. Tittsworth, N. Moelders, and P. J. Schilling, J. Synchrotron Radiat. **6**, 588 (1999); I. Winter, J. Hormes, and M. Hiller, Nucl. Instrum. Methods Phys. Res. B **97**(1–4), 287 (1995).
[10]T. A. Smith, J. G. Dewitt, B. Hedman, and K. O. Hodgson, J. Am. Chem. Soc. **116**(9), 3836 (1994).
[11]M. Howells, C. Jacobsen, T. Warwick, and A. Bos, *Science of Microscopy* edited by P. W. Hawkes and J. C. H. Spence (Springer, New York, 2008), Chapter 13, pp. 835–926; G. Van der Snickt, J. Dik, M. Cotte, K. Janssens, J. Jaroszewicz, W. De Nolf, J. Groenewegen, and L. Van der Loeff, Anal. Chem. **81**(7), 2600 (2009); M. Cotte, E. Welcomme, V. A. Sole, M. Salome, M. Menu, P. Walter, and J. Susini, *ibid.* **79**(18), 6988 (2007); J. Prietzel, J. Thieme, U. Neuhausler, J. Susini, and I. Kogel-Knabner, Eur. J. Soil. Sci. **54**(2), 423 (2003); K. L. I. Norlund, G. Southam, T. Tyliszczak, Y. F. Hu, C. Karunakaran, M. Obst, A. P. Hitchcock, and L. A. Warren, Environ. Sci. Technol. **43**(23), 8781 (2009).
[12]K. V. Kaznatcheev, C. Karunakaran, U. D. Lanke, S. G. Urquhart, M. Obst, and A. P. Hitchcock, Nucl. Instrum. Methods Phys. Res. A **582**(1), 96 (2007).
[13]C. Dezarnaud, M. Tronc, and A. P. Hitchcock, Chem. Phys. **142**, 455 (1990).
[14]C. Dezarnaud, M. Tronc, and A. Modelli, Chem. Phys. **156**(1), 129 (1991); A. P. Hitchcock, S. Bodeur, and M. Tronc, Physica B **158**(1–3), 257 (1989); R. Chauvistre, J. Hormes, E. Hartmann, N. Etzenbach, R. Hosch, and J. Hahn, Chem. Phys. **223**(2–33), 293 (1997); J. Phys. Colloque, T47, C8-575 (1896).
[15]A. Mijovilovich, L. G. M. Pettersson, F. M. F. de Groot, and B. M. Weckhuysen, J. Phys. Chem. A **114**(35), 9523 (2010).
[16]R. Sarangi, P. Frank, K. O. Hodgson, and B. Hedman, Inorg. Chim. Acta **361**(4), 956 (2008).
[17]A. Mijovilovich, L. G. M. Pettersson, S. Mangold, M. Janousch, J. Susini, M. Salome, F. M. F. de Groot, and B. M. Weckhuysen, J. Phys. Chem. A **113**(12), 2750 (2009).
[18]E. D. Risberg, F. Jalilehvand, B. O. Leung, L. G. M. Pettersson, and M. Sandstrom, Dalton Transactions **18**, 3542 (2009).
[19]H. Nakamatsu, T. Mukoyama, and H. Adachi, J. Chem. Phys. **95**(5), 3167 (1991).
[20]S. Bodeur, A. P. Hitchcock, and N. Kosugi, Chem. Phys. **162**(2–3), 293 (1992).
[21]E. Damian, F. Jalilehvand, A. Abbasi, L. G. M. Pettersson, and M. Sandstrom, Phys. Scr., T **115**, 1077 (2005).
[22]E. D. Risberg, L. Eriksson, J. Mink, L. G. M. Pettersson, M. Y. Skripkin, and M. Sandstrom, Inorg. Chem. **46**(20), 8332 (2007).
[23]R. A. Mori, E. Paris, G. Giuli, S. G. Eeckhout, M. Kavcic, M. Zitnik, K. Bucar, L. G. M. Pettersson, and P. Glatzel, Anal. Chem. **81**(15), 6516 (2009); R. A. Mori, E. Paris, G. Giuli, S. G. Eeckhout, M. Kavcic, M. Zitnik, K. Bucar, L. G. M. Pettersson, and P. Glatzel, Inorg. Chem. **49**(14), 6468 (2010).
[24]J. A. Tossell and D. J. Vaughan, J. Colloid Interface Sci. **155**(1), 98 (1993); J.-I. Adachi, Y. Takata, N. Kosugi, E. Shigemasa, A. Yagishita, and Y. Kitajima, Chem. Phys. Lett. **294**(6), 559 (1998).
[25]F. A. Gianturco, U. Lamanna, and C. Guidotti, J. Chem. Phys. **57**(2), 840 (1972); C. Reynaud, S. Bodeur, J. L. Marechal, D. Bazin, P. Millie, I. Nenner, U. Rockland, and H. Baumgartel, Chem. Phys. **166**(3), 411 (1992).
[26]N. Kosugi, Theor. Chim. Acta **72**(2), 149 (1987); N. Kosugi and H. Kuroda, Chem. Phys. Lett. **74**(3), 490 (1980).
[27]R. R. Cooney and S. G. Urquhart, J. Phys. Chem. B **108**(47), 18185 (2004).
[28]E. Otero and S. G. Urquhart, J. Phys. Chem. A **110**(44), 12121 (2006); K. Ueda, M. Okunishi, H. Chiba, Y. Shimizu, K. Ohmori, Y. Sato, E. Shigemasa, and N. Kosugi, Chem. Phys. Lett. **236**(3), 311 (1995); S. G. Urquhart and H. Ade, J. Phys. Chem. B **106**(34), 8531 (2002).
[29]S. G. Urquhart, C. C. Turci, T. Tyliszczak, M. A. Brook, and A. P. Hitchcock, Organometallics **16**(10), 2080 (1997).
[30]S. G. Urquhart, A. P. Hitchcock, J. F. Lehmann, and M. Denk, Organometallics **17**(11), 2352 (1998).
[31]S. G. Urquhart, A. P. Smith, H. W. Ade, A. P. Hitchcock, E. G. Rightor, and W. Lidy, J. Phys. Chem. B **103**(22), 4603 (1999).
[32]E. Otero, N. Kosugi, and S. G. Urquhart, J. Chem. Phys. **131**, 114313 (2009).
[33]J. F. Lehmann, S. G. Urquhart, L. E. Ennis, A. P. Hitchcock, K. Hatano, S. Gupta, and M. K. Denk, Organometallics **18**(10), 1862 (1999).
[34]SPARTAN, Wavefunction, Inc., Irvine, CA, 1994.
[35]B. Huo, A. P. Hitchcock, *Simile2*, McMaster University, Hamilton, ON, 1996.
[36]A. P. Hitchcock and M. Tronc, Chem. Phys. **121**(2), 265 (1988).
[37]M. Breinig, M. H. Chen, G. E. Ice, F. Parente, and B. Crasemann, Phys. Rev. A **22**(2), 520 (1980).
[38]See supplementary material at http://dx.doi.org/10.1063/1.3602218 for a summary of literature calibrations at the sulfur 1*s* energy.

Downloaded 21 Feb 2012 to 128.233.108.204. Redistribution subject to AIP license or copyright; see http://jcp.aip.org/about/rights_and_permissions